Vavřík *et al. Heritage Science* (2024) 12:87
https://doi.org/10.1186/s40494-024-01202-8

Heritage Science

RESEARCH

Open Access

# The use of computed tomography and X-ray fluorescence analysis in the research of printed book from the seventeenth century: book binding, tomographic reading of the text, dendrochronological dating, pigments analysis

Daniel Vavřík[2*], Andrei Kazanskii[1], Jitka Neoralová[1], Rita Lyons Kindlerová[1], Dana Novotná[1], Petra Vávrová[1], Ivana Kumpová[2], Michal Vopálenský[2] and Tomáš Kyncl[3]

**Abstract**

This paper presents the use of X-ray computed tomography and X-ray fluorescence in the analysis and expert research of the seventeenth century printed book "Eukhologīon albo Molitoslov, ili Trebnik" from Kiev. The main purpose of the survey was to confirm whether the book binding is original or whether it is a rebinding, and whether there are any fragments of the hidden older texts. Commonly used radiography is usually not able to provide sufficient information for these purposes. On the other hand, computed tomography allows a detailed and three-dimensional documentation of the bookbinding technology and the structure of the materials used, including the wooden boards. It will be presented that all elements of the weave are clearly visible, making it possible to show that there are no internal defects in the stitching and materials. It has also been convincingly shown that there are no fragments or layers of older texts in the binding, so no further invasive intervention will be necessary regarding this aspect. The paper also demonstrates the possibility of reading the text in a closed book utilising X-ray computed tomography data; this option may be advantageous for massively damaged manuscripts. It will also be shown, that thanks to detailed tomographic imaging of the wood structure of the boards, a dendrochronological survey can be successfully carried out without invasive intervention into their outer layers. From the CT data it was also found that the pigments of the letters have significantly different densities. Therefore, as part of the survey, elemental analysis of the writing was also carried out using a portable X-ray fluorescence spectrometer to confirm and clarify this finding.

**Keywords** X-ray computed tomography, Book binding, X-ray fluorescence analysis of paper and ink, Dendrochronological book dating, Tomographic text reading

*Correspondence:
Daniel Vavřík
vavrik@itam.cas.cz
[1] National Library of Czech Republic, Klementinum 190, 110 00 Prague 1, Czech Republic
[2] Czech Academy of Sciences, Institute of Theoretical and Applied Mechanics, Prosecka 809/76, 190 00 Prague 9, Czech Republic
[3] DendroLab Brno, Eliasova 37, 616 00 Brno, Czech Republic

## Introduction

Historical prints and manuscripts contain a lot of information about their origin, creators and owners. In addition to the materials used, related to book binding construction, printing and decorative techniques, the history of book has been imprinted in its deterioration and various defects over the years. In this context, previous restoration interventions that may not have been

documented can be expected. In addition, fragments of older parchment manuscripts are quite commonly present in the binding; [1] states that up to 20% of the manuscripts contain such pieces.

A number of inspection techniques are used to study not only the above aspects, and the applicability of each technique depends on the problem under study. For example, if the page is directly accessible, UV light, Multi- and Hyperspectral Imaging (MSI, HIS) can be used to discover previously erased and overwritten text [2–5]. The distribution map of elements in the illumination can be probed with macro-X-ray fluorescence (XRF), while the underpainting can be investigated with infrared (IR) imaging [6]. Investigation of iron-gall ink corrosion and its components' migration into the surrounding material can be performed using micro- (XRF) analysis [7] or by the scanning transmission X-ray microscopy [8].

A completely different situation regarding the applicability of the inspection techniques occurs when the feature under investigation is not directly accessible. For example, the identification and reading of text hidden in a parchment binding can be done by XRF techniques, but only if the other covering material does not block soft X-rays [1, 11]. In some cases, such as the interlayer between end paper and board, active IR thermography can be used to investigate hidden subsurface structures [10]. Due to its nature, X-ray computed tomography (CT) is a very suitable tool for exploring hidden structures and is already widely used for various tasks. The possibility to document rebinding using micro CT has been shown in [11]. Recently, the identification and reading of parchment fragments hidden in a binding has been successfully tested using a medical CT scanner [12], but it has been noted that only text containing heavy elements (mercury in this case) is visible, whereas printing with carbon-based ink is not. A similar conclusion was reported in [13], where a method of reading text inside a closed manuscript was tested—iron and mineral-based inks are visible by X-ray, whereas carbon-based inks are not. Recently, it was possible to read a few words from a carbonized scroll of Herculaneum papyrus that were written with carbon-based ink [14]. However, the text only became visible using phase contrast tomography, which is based on a different principle than standard CT.

Note that the X-ray attenuation contrast between the two materials, which is the essence of CT structure resolvability, is primarily based on the difference in their elemental composition (and secondarily on the difference in their porosity). Therefore, the X-ray attenuation contrast between two organic materials, such as a support and a carbon-based ink, is relatively low. In principle, however, the contrast between the substrate and the text can still be sufficient for detection if a very low energy X-ray spectrum is used. Unfortunately, such a requirement is inconsistent with tomography of relatively massive objects, such as thick mediaeval leather bound books with wooden boards to boot—the soft part of the X-ray spectrum is almost completely attenuated.

The object chosen for the research is a historical book printed on paper included in the collection of the Slavonic Library, originally from Kiev from 1646, the full title of which is *Eukhologīon albo Molitoslov, ili Trebnik* (short title *Euchologion*), better known as *Trebnyk Petra Mohyly*. The book became the subject of the research because of the number of marginalia and attributions, especially from other owners, that tell about the places where the book went. Due to the interesting narrative associated with the book, the bookbinding was subjected to research aimed at finding further evidence of its history and use.

The main aim of the research presented in this paper was to confirm whether the book has an original binding or rebinding and whether the binding contains fragments of older texts. Radiography could not resolve these questions. Therefore, X-ray computed tomography was performed. In addition to visualising the various parts of the book binding to obtain answers, dendrochronological dating of the wooden boards was carried out on the basis of the tomographic data. Also the ability to read the closed books was tested; similar to other referenced works, some parts of the text were readable, some in practice were not. To clarify this finding, it proved beneficial to determine the composition of the inks used by X-ray fluorescence analysis.

## Petro Mohyla's *Euchologion* (1646)

The book comes from the Kyiv Monastery of the Caves, where it was prepared and edited by theologian Petro Mohyla (1597–1647). Its owners were members of the Krasilnikov family. They are assumed to have received it in return for services rendered, but it is not known what those services were. Book consists of three parts. Part I contains the rites for the celebration of the Sacraments and the most important prayers related to the life of a Christian from birth to death. Part II contains the rites for the consecration and blessing of various church and household items. Part III contains supplications for events concerning the lives of individual Christians or communities. As can be seen visually, these parts were made of different paper (hence a different chemical composition may be expected), but from the beginning they were bound into one single bundle. A digital copy of the book with further details is available at [15].

The external dimensions of the book are 235 × 333 × 120 mm, the 1566-page block measuring 212 × 313 × 104 mm. The bookbinding's cover is completely of leather, with about 10 mm thick wooden boards featuring brass clasps. The book block it self is made up of

**Fig. 1** View of the book block and fittings from the side of the backboard

hand-stitched signatures. The book block is sewn on double raised cords, with a slightly rounded spine (Fig. 1). The end bands near the head and tail were laced through the exterior face of the board, with the remaining two central bands glued to the end paper under the pastedown. The end papers are made of double leaves, one of which is pastedown with hooked leave. The board cover is made of tanned leather and is mechanically damaged, especially in the area of the spine. Despite the damage, the blind stamped decoration on the board cover and spine is still noticeable. There are stains on the leather. It is difficult to determine whether this is damage or artistic intent. The brass clasps also consist of metal parts (such as catch plates on the back board) that are not the same. Probably one of them was added later, but it is not possible to determine which. The bodies of both clasps have shaped ends and are decorated with simple chasing. One of the clasps is fixed to the strap with a modern iron nail. The edge was originally coloured. Sewn headband and tailband have survived. Red and black printing was used in the book block.

## Methods: X-ray computed tomography

One of the basic techniques used to investigate the internal structure of objects is radiography, in which transmitting X-rays through the object are registered by a detector behind it. The intensities of a two-dimensional X-ray image are related to the attenuation of X-rays by the object along the lines connecting the detector pixels with the X-ray source. Therefore, such an image does not provide information about the spatial arrangement of the internal object features. However, such information can be revealed by means of X-ray computed tomography (CT).

The dataset required for a CT reconstruction consists of a set of X-ray images which are recorded during the relative rotation of the object to the X-ray—detector system (within the context of tomography, these X-ray images are called projections). In our case, the tested sample rotated and the X-ray—detector system remained in a fixed position. The X-ray—sample—detector distance ratio defines the projection magnification. During CT reconstruction, all projections are virtually back-projected across the reconstructed volume after application of a high-pass filter, resulting in a tomographic volume [16]. With a sufficient number of projection angles, faithful information is obtained about the external geometry of the examined object and its internal structure. Depending on the required reconstruction quality, hundreds or thousands of projection angles may be needed.

The Twinned Orthogonal Adjustable Tomograph (TORATOM) research scanner at the Telč Centre allowing a wide range of various tomographic modalities [17, 18] was used for this work employing the imaging line with microfocus X-ray tube. The scanner the scanner is in- house-developed experimental device patented on the European level [19]. It comprises computer-controlled axes positioning for setting "X-ray—sample—detector" distances. This makes it possible to change the magnification from about 1.2× to 100×. With available detectors, it is possible to achieve resolutions of CT reconstructions at the spatial element scale (voxel, which can be taken as 3D pixel) from units up to two hundred micrometres.

### Safety of X-ray methods for manuscript research

As part of the NAKI II[1] project entitled “Use of Imaging Techniques for Studying Hidden Information in Books”, the National Library of the Czech Republic focused on the safety of book research using X-rays. The tests followed earlier published research into the irradiation of paper samples on the basis of synchrotron (SR-X radiation), macro XRF, etc. The X-ray doses were in the range of 3.5–20 Gy during the tests on the samples [20], when monitoring cellulose chain cleavage and hydroxyl free radical formation using chromatographic separation techniques (SEC-MALS-DRI and RP-HPLC-FLD-DAD), characterized the optical properties of the paper by spectroscopy (UV luminescence and diffuse reflectance). The

[1] NAKI—Program of Applied Research and Development of National and Cultural Identity (Ministry of Culture of the Czech Republic).

results of the measurement of the change in the degree of polymerization showed no macromolecular defects in the paper samples. There was also no impact on the optical properties of the paper samples. Changes at the macromolecular level began to manifest themselves at doses higher than 1 kGy. Similar conclusions regarding the safety of X-ray book can be found in [21] for book printed on paper and in [22] for books printed on parchment respectively. Moreover, historical paper was shown to have a higher resistance to X-rays than modern archival paper [23]. In the National Library of the Czech Republic, tests were carried out on the effect of X-rays on paper at 120 kV voltage and 0.3 mA current with X-ray tube distance of 790 mm from the detector, paper was placed near to the detector. Three different irradiation times were applied, namely 10, 30 and 60 min. The measurements showed that the longest exposure yielded a dose of 0.3 Gy. This measurement was done by the calibrated dosimeter. Note that this value is related to the human body, but it can be taken as appropriate as it has similar density as a paper. In accordance with the above referenced works, no change in colour, mechanical properties or pH was observed in any of the samples tested within the NAKI II project [24] (in Czech).

### Description of X-ray CT measurement

The book was placed in a protective case, a box made of alkaline sandwich cardboard, which is secured against opening by adhesive tape throughout the recording of tomographic data. The box was placed on a turntable with the longest side of the book held vertically. A microfocus X-ray tube (XWT-240-TCHR, X-Ray WorX, Germany) operating in microfocus-mode, with a working voltage of 180 kV and a target current of 860 mA, i.e. power of 155 W, was used for tomographic scanning. In order to optimise the spectrum of the X-ray source, a filter consisting of 4 mm Al and 1.5 mm brass was installed in front of the tube head. A flat panel (XRD-1622-AP-14, Perkin Elmer, DE) with an active area size of 409.6 × 409.6 mm, a pixel matrix of 2048 × 2048 with 200 µm pixels, operated with a capacity of 0.5 pF and an exposure time of 3 × 1.2 s (averaged), was used for imaging. The detector positioned at a distance of 1340 mm from the X-ray tube spot; the object at a distance of 1200 mm from the tube, achieving a geometric magnification of 1.1×, resulting in a intirstic voxel size of 179 µm in reconstruction. To achieve higher intrinsic spatial resolution for such a relatively large object would require a larger detector and/or a detector with smaller pixels. A total of 1800 projections were recorded during 2:30 h (the total exposure plus the time needed for all rotations of the CT stage). Standard dark-field and flat-field corrections were used to correct the projections, using images averaged from 150 with the exposure time of 1.2 s. The tomographic scanning parameters resulted in a total dose of 0.63 Gy (obtained using a dosimeter), which is close to the reference measurement and well below the parameters listed in [23]. It can be therefore concluded, that no measurable damage to the examined manuscript occurred.

The resulting 3D tomographic model was reconstructed using filtered back projection in VGStudio MAX 3.2. For the purpose of demonstrating the possibilities of reading a closed book based on tomographic data, the oversampling method for obtaining more detailed information was tested, see the Sect. "Testing the ability to read a closed book based on tomographic data".

### Evaluation of tomographic data

The information that could be learned from the book's binding by direct observation was significantly broadened due to the tomographic research. A binding is a combination of different materials, from those with low X-ray attenuation (i.e. with low density) such as paper, textiles and leather, through those that are more attenuating, such as wood, to those that are highly attenuating, such as dense metals. In general, regarding the evaluation of tomographic data, the 3D tomographic model represents the spatial distribution of the calculated CT densities of the object under study. This gives an idea of the structure and shape of the object as well as indirect information about its chemical composition. The CT densities are represented by a histogram in the corresponding visualization software (VGStudio MAX 3.2 in our case). By manipulating this histogram appropriately, we can highlight different parts of the model with different densities. The virtual model can then be examined in different ways. The basic one is to display its section laying in the selected geometric plane. Furthermore, the model can also be displayed in a three-dimensional representation, or in combination with a section. The choice of how to display the tomographic model depends on what we want to investigate in the object. In the following sections we will show some examples of the visualization of different elements of the book.

#### *Binding structure, materials, accessories and decoration*

A very useful tool for viewing the internal structures of the book is the 3D visualization of the tomographic model. This makes it possible, for instance, by rotating the visualization to determine the method of stitching, binding and layering. Note that the initial overall observation is very important subsequently for the proper orientation of the sections of the model. Navigating individual sections from different angles can be confusing for the observer and lead to misidentification of the location of the element being studied. The tomographic model

enables the investigation of the condition of the thread, and its integrity throughout the book block can therefore be thoroughly checked.

The ornamental gilding on the spine, including the text and lines between the raised bands, can be seen in Fig. 2, which shows a 3D tomographic view of the "semi-transparent" spine of the book. Some high-density particles hidden in the spine of the book, which are not optically visible on the outer surface, appear as white lines and dots in this image. Their composition cannot be determined by XRF because they are not directly accessible.

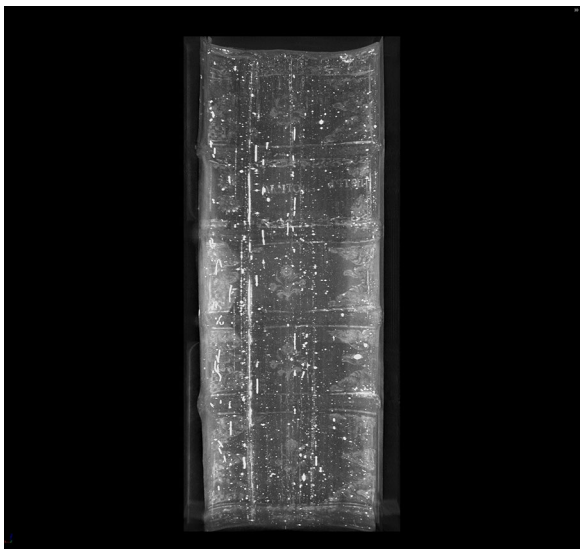

**Fig. 2** Tomographic view of the "semi-transparent" spine of the book

Figure 3A, the visualization was set to highlight the structure of the spinal sewing stations, which each consists of (two) lengths of twisted cord. Images of the sections in the plane of the book boards did not reveal the use of labels or secondary materials under the leather covering. In Fig. 3A, the wooden board with the glued ends of the cords are clearly visible. In Fig. 3B, the annual rings in the wood are clear and the holes for cords are free of any damage that would be expected if restringing had been done in the past. Figure 3C shows 3D visualization with reduced visibility of lighter elements, highlighting instead details of the lettering containing heavy elements, sewing stations, and clasps.

In Fig. 4 A, a detail of the longitudinal section through the spine is shown in Fig. 4 B—the layers of the box in which the book was placed are visible on the right (c). In close proximity to the material of the box is the compact layer of the leather cover, which is no longer glued to the entire length of spine, but which is noticeable in the space between the bands of the cavity. The leather fits tightly against the protruding bands. We see a cut through the individual bands, which are formed by two cords wrapped around a thread. The passage of the thread through the paper is also visible. In Fig. 4C, horizontal (axial) passing through the holes through which the ends of the cords are passing (e). Red text appears

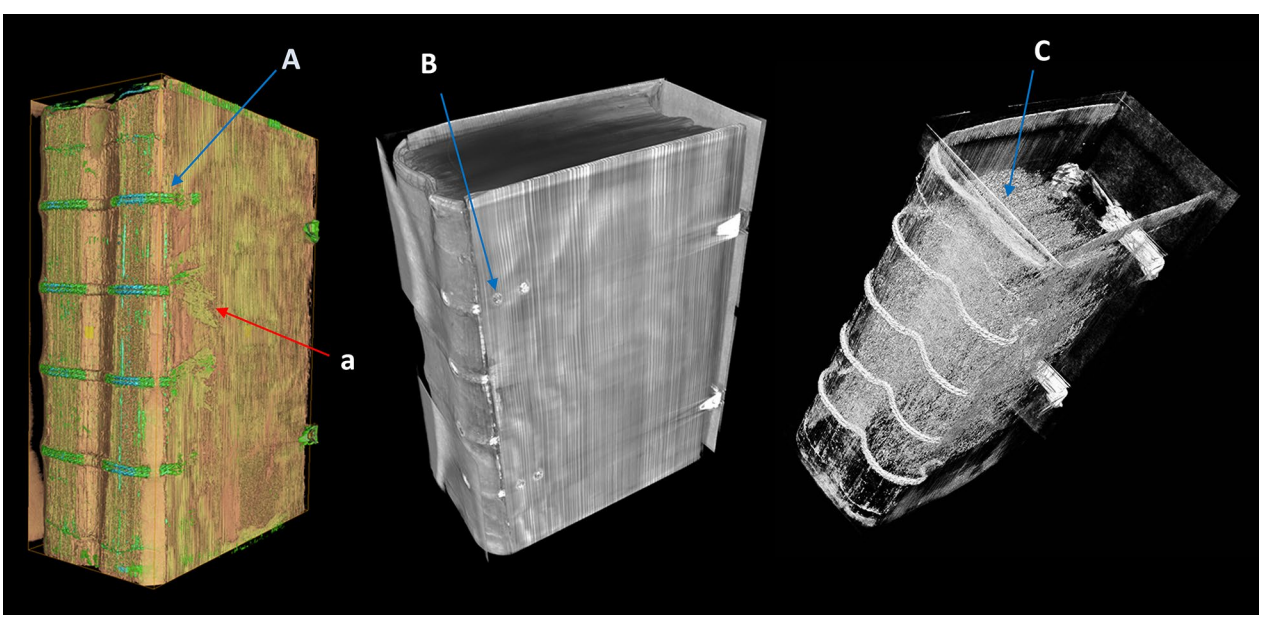


**Fig. 3** **A** Tomographic view of wooden boards and book spine with sewing stations (indicated by blue arrow), **a** glued ends of the cord; **B** annual rings in boards pronounced, sewing non-damaged holes clearly visible (arrow); **C** visibility of lighter elements suppressed, block of letters containing heavy elements (arrow), book bindings and clasps highlighted

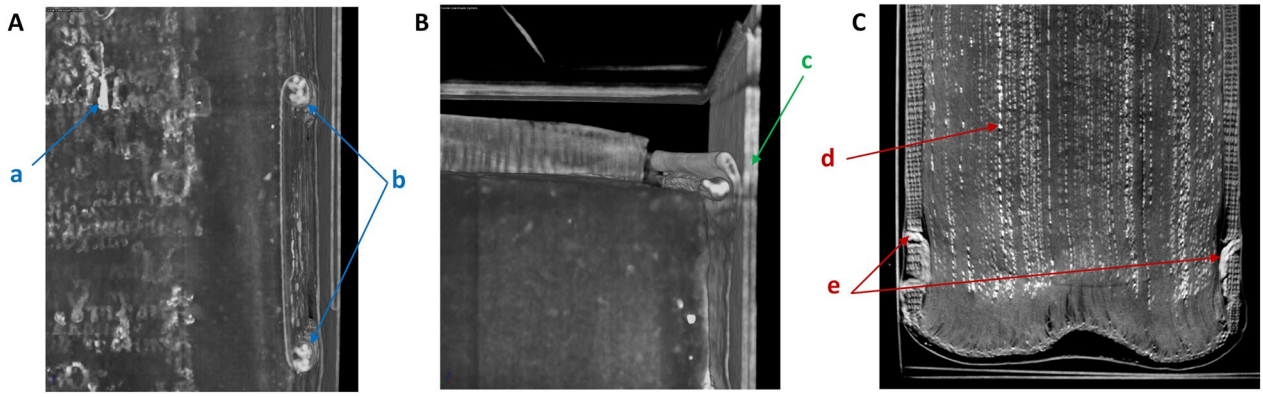


**Fig. 4** **A** Detailed section of spinal binding, visible font is labelled by **a** and twisted cords by **b**; **B** 3D visualization of the headband, paper box wall is labelled by **c**; **C** Axial section, arrow with **e** is showing cords passing thought the wooden boards, **d** red letters are manifested as white dots

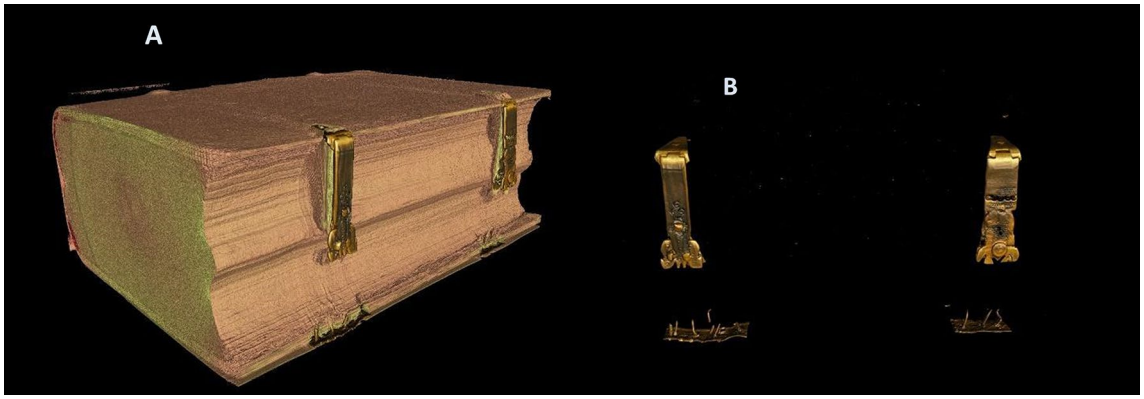


**Fig. 5** **A** Whole book; **B** Separated clasps where small nails are visible

as white dashed lines (d), while the other leaves are in shades of grey. The text is visible due to the high elemental differentiation of the historical red colour, with its high mercury content; similar pigment is described in [25]. With the correct choice of angle and position of the section, the text can be read in parts. However, this is complicated by the considerable waviness of the pages. The possibility of a more comfortable tomographic reading of the pages of a closed book will be shown in the following section, "Testing the ability to read a closed book based on tomographic data".

Note that if the binding was repaired, the book block would show holes from the original stitching and probably also thread remnants. Possibly glue residue and ends of frayed twine would be visible on the wooden boards. Nothing of the above was discovered during a careful examination of the CT volume. No parts are visible on the wooden boards indicating the earlier layers of attachment of the book boards. No distinct layers are visible in the spine to indicate the presence of fragments of recycled materials.

The images in Fig. 5 document the shape of the metal clasps. The 3D visualization of the whole book (A) with the setting to highlight the metal elements (B) shows the possibility for the different materials to be documented separately.

### *Testing the ability to read a closed book based on tomographic data*

In addition to studying the construction of the book, an interesting option is to read the text in a closed book on the basis of tomographic reconstruction. In the case presented here, this is not necessary. However, in rare book collections there are a number of books (or scrolls and other documents) that are difficult or impossible to be opened (unpacked) due to their current state [26]. Not many papers have been published on this topic, with those that have mostly presented simpler cases in which the pages do not overwhelm each other [27], or, in the

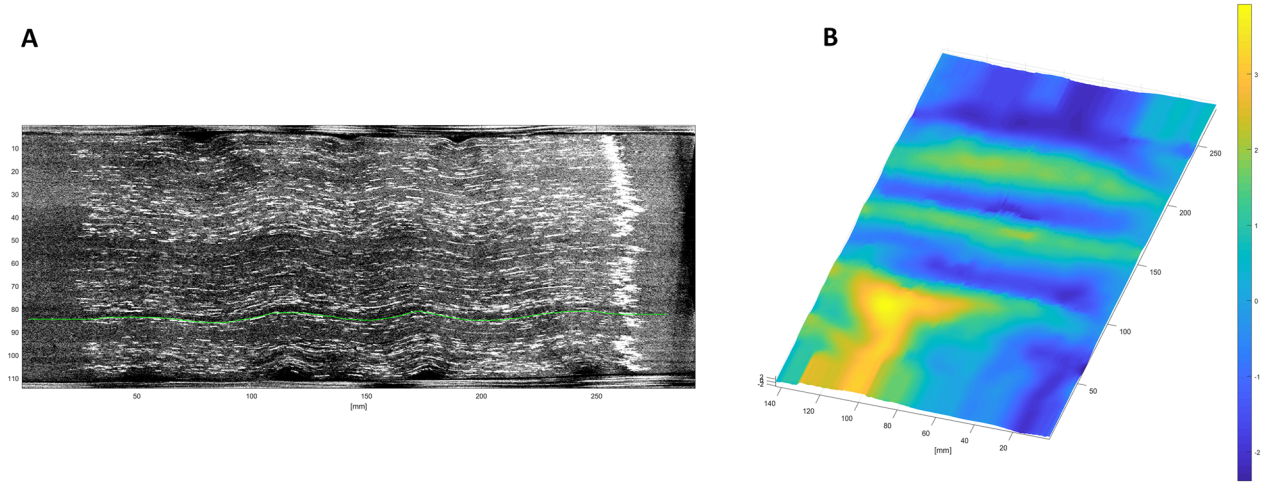


**Fig. 6** **A** Section of book block, spine is left. The green line in the book block indicates the found edge of the page. **B** imaging of the sheet waviness

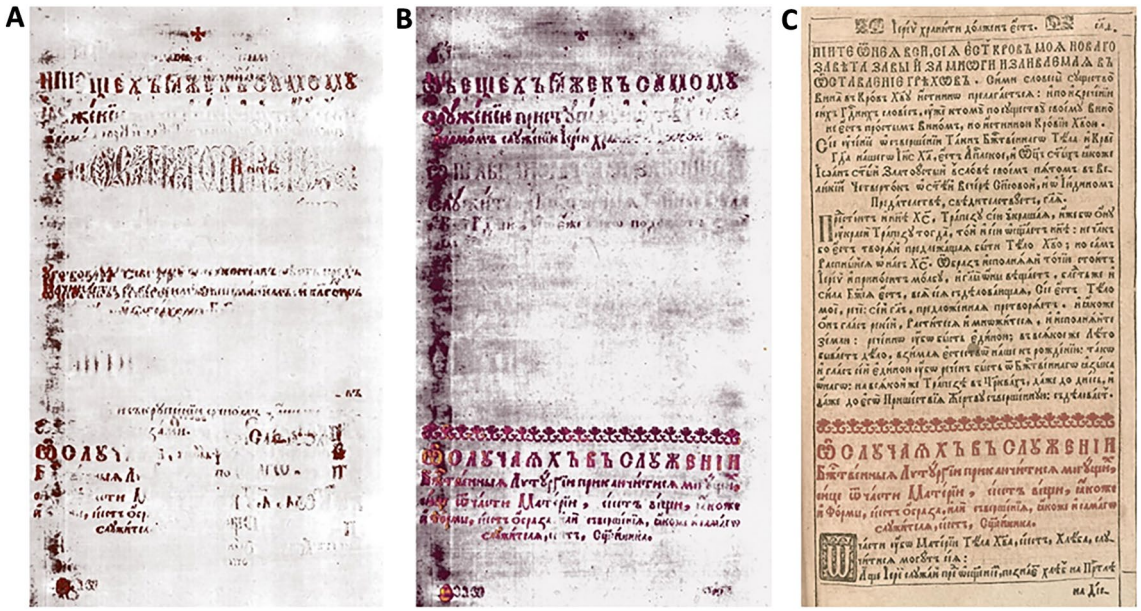


**Fig. 7** **A** Tomographic display of text before virtual straightening; **B** text from relatively distant places in the book is visible after straightening. On the right **C** is the image of page 239 of the first pagination

case of denser book blocks, only small fragments of text have been read, see [11–14].

In the case of reading closed books by means of tomographic reconstruction, we are faced with the problem that, especially in old imprints, the pages are wavy, while it is most convenient to examine the tomographic volume in its planar sections. However, if the pages are wavy, we will see text coming from different pages in the given section, see Fig. 7A. In Fig. 6 is a sample of a section of a book block, perpendicular to the pages (the book is lying as if on a board). The white colour represents the highly attenuating red pigment, while the grey colour corresponds to sheets with only black pigment, which does not create any contrast. The page waviness exceeds 6 mm, which in this case includes 50 pages of text (including air gaps between pages), due to which an unclear mismatch of text can be seen in one planar section of the initial CT reconstruction that is very difficult to navigate.

Since the initial voxel size was larger than the page thickness in the reconstruction discussed above, the book was reconstructed with a voxel size 4 times smaller in the direction perpendicular to the pages, in order to

separate the information for each sheet. The resulting voxels are 45 × 179 × 179 μm. It should be emphasized that the voxel size is defined before CT reconstruction and can therefore be smaller than the size given by the pixel size divided by the magnification as is usual, so it is not a simple division of voxels into smaller ones on the already performed CT reconstruction. To improve the voxel size, several conditions must be met: the number of projections is high enough, the scatter is not too pronounced and the object structure has good contrast. In our work, it was verified by traversing the reconstructed volume that the change in structure is well visible even when the movement is equal to the voxel size. If the voxel size improvement had failed, these changes would not be visible.

The book block was reconstructed with four times smaller voxels in one direction only, because it already represents $8 \times 10^9$ voxels and increasing the resolution in all directions would have created problems in handling the data. Moreover, it would not bring any new information, only the inevitable increase in noise complicating the search for red letters.

The next step involved virtual page straightening. First, it was necessary to find a surface describing the shape of the selected page of the book. This was implemented as follows: In the selected section, Fig. 6A, the approximate position of seed letter (which appears as a white line in the section) in the middle of the edge of the reference page is selected by the mouse. Its position is refined automatically by software searching for a maximum density voxel in a small, predefined area. Likewise, the next character is searched (approximately) in the direction of the line of the text (x-direction in Fig. 6A) within a defined area, at a distance roughly corresponding to the letter pitch of the text. Once the positions of at least three letters are known, additional characters are searched on the basis of the extrapolation curve passing through the previously found characters. By finding all the characters over the full width of the book block, we get the shape of the sheet a curve describing the shape of the page in the given section, see the green line in the book block at the in Fig. 6 A. In the part outside the area containing red letters, this curve is extrapolated from the last character found. The found curve then serves as the initial condition for finding the page shape in adjacent sections (towards the text lines of text). Using the procedure described in [28], the entire shape of the page is finally found, see Fig. 6B. This figure shows that the page has a wave range of 6.7 mm.

In the last step, the book block was virtually straightened according to this found area. Basically, this involves the transformation of the coordinate system, see [28] and [29] for more details, which is defined according to the page shape found. The result is significantly improved readability of the text. Figure 7 shows (A) a tomographic section before straightening, (B) a page after straightening (this is page of book 239), and (C) a photo of the same page on the right for comparison. Note that the page has not been perfectly straightened, so we still see text from different pages, although at a range about 10 times smaller than without straightening. The main reason for the imperfect straightening is the fact that some areas without tomographically visible text exist on the entire reference page, so that during the search for the page area there are "jumps" to adjacent pages. Even so, the result is considerably clearer than in the initial state.

To make the procedure easier to explain and to make the result easy to read, a sheet with text in red ink on one side only has been selected here. In the case of double-sided sheets printed in red ink, the text on both sides is together in a straightened sheet. Although in such a case it is relatively easy for an experienced reader to separate the text from both sides based on context, further work will be needed to automate the whole process, based on a different (linguistic) principle than presented here.

Similar results from virtual straightening can, of course, be presented for other pages of the book. Since the waviness of the book pages are not uniform throughout the book block, the presented virtual flattening is valid only locally, i.e. for several neighbouring pages. If it is required to read the entire book without opening it, the above procedure will have to be repeated for the other pages at intervals of several pages. On the other hand, the first found page shape will be able to serve as an initial condition for automating the process of reading the whole book. It can be assumed that the correct identification of text on individual pages will need to be improved on a linguistic basis. If the textual context is lost, the correct page shape will have to be searched in the vicinity until the textual context is found again. Nevertheless, it has been shown here that it is possible to apply the algorithm to highly wavy pages that would otherwise be very difficult to read directly from the non-processed tomographic model.

#### *Dendrochronological analysis of book covering*

Dendrochronological analysis was performed from the tomographic model of the wood rings on the book boards in order to date them, see [30] for similar work. The sections of the left and right wooden boards in the tomographic model were used, see Fig. 8A and B. Only the boards were reconstructed with four times smaller voxels, similar to the previous section, but in all dimensions (i.e. 45 × 45 × 45 μm) to improve the identification of the wood year rings. The images provided important information about the width of the tree rings and their

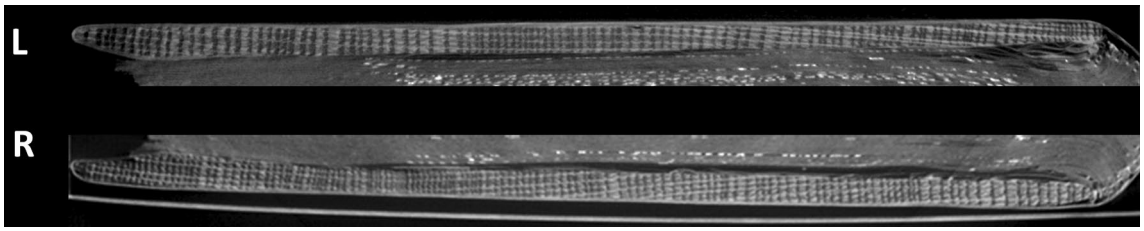


**Fig. 8** Cross-section of the wooden left (L) and right (R) book board

number. It was proven to be oak wood by comparing thirteen CT sections for each book board with the appearance of oak under optical microscopy. The basic features are clearly visible from the CT examination.

The determination of the age and species of the wood was performed using common xylotomy methods [31]. The dendrochronological processing method was divided into several steps and followed the standard chronology of tree ring widths [32, 33]. First, the width of the tree rings on X-ray tomography images was measured using OSM32 (www.sciem.com). Subsequently, relative synchronisation of the obtained tree-ring series was performed. The ring curves were then compared and relatively synchronised. The sets of mutually synchronous curves were averaged into sum curves. The last step was to attempt absolute dating using the PAST program (www.sciem.com). This program includes data verification and synchronization of tree-ring series with standard chronology. When using this program, the degree of similarity of the compared series or chronology is assessed using the correlation coefficient and the concurrency coefficient (Gleichlaufigkeit) after standardisation using Hollstein high-frequency filters and the Baillie & Pilcher method [34]. Available standard oak chronologies for Central Europe, France, Poland and the Baltics were used to date the oak. The attempt at relative synchronization of the ring curves of the two book boards was not successful. The book boards were therefore dated separately. Absolute dating of tree ring curves with standard oak chronologies resulted in the discovery of a synchronous position in only one row. This curve was reliably datable to the 2021BLT1 and 2021BLT3 chronologies, which represent oak material originating in the Baltics [35]. These particular chronologies probably represent oak trees originating in the area of present-day Lithuania [35]. A tree ring dating back to the year of felling of the used trees has not been preserved on either of the book boards. In these cases, therefore, it was only possible to equivocally identify the earliest year after which the used tree was cut, namely after 1608, which corresponds to the preserved historical information about the book and confirms the originality of the preserved book boards [36], [37].

## Methods: investigation of chemical composition of inks based on X-ray fluorescence

X-ray fluorescence (XRF) is an important non-destructive method for investigating the chemical composition of materials including medieval manuscripts [38–40]. The object under investigation is irradiated by X-rays (or gamma rays), which excites electrons in atomic shells into higher layers. Deexcitation occurs, i.e. the return of electrons to the inner layer. This releases energy in the form of electromagnetic radiation, whose wavelength or spectrum is characteristic for every chemical element. The energy of the emitted photons is relatively low, so there is strong attenuation in the material being studied. This fact represents a major limitation of this method because secondary photon attenuation makes it impossible to perform analysis at greater depths of the material. However, this fact does not pose a significant obstacle to measuring the composition of the inks in the directly visible pages of the historical book.

### Description of the XRF measurement

A Prospector 3 handheld spectrometer manufactured by Elvatech Ltd. was used for the XRF spectrometric measurements. This device is equipped with X-ray tube with a rhodium anode, with a maximum current of 200 μA and an acceleration voltage of up to 50 kV. Prospector 3 has energy resolution of 140 eV at the Kα line of manganese.

The book was supported by soft wedges to avoid excessive stress on the bookbinding when it was opened. XRF data were collected from five pages, in which mostly an area of only one colour was taken, but in one case both colours on the same side. An ink-free area, i.e. blank paper, was always taken as a reference sample. A collimator with a diameter of 2 mm was used for all the measurements. The measured area was targeted using an image from an integrated camera. Data acquisition was always carried out in two steps. In the first step, data suitable for emission edge analysis at higher energies (up to 35 keV, so-called "heavy spectrum") were collected. The data acquisition took 200 s, with an integrated 0.8 mm thick aluminium filter placed in front of the X-ray source. In the following step, data suitable for more sensitive spectrum analysis in lower energy regions were collected

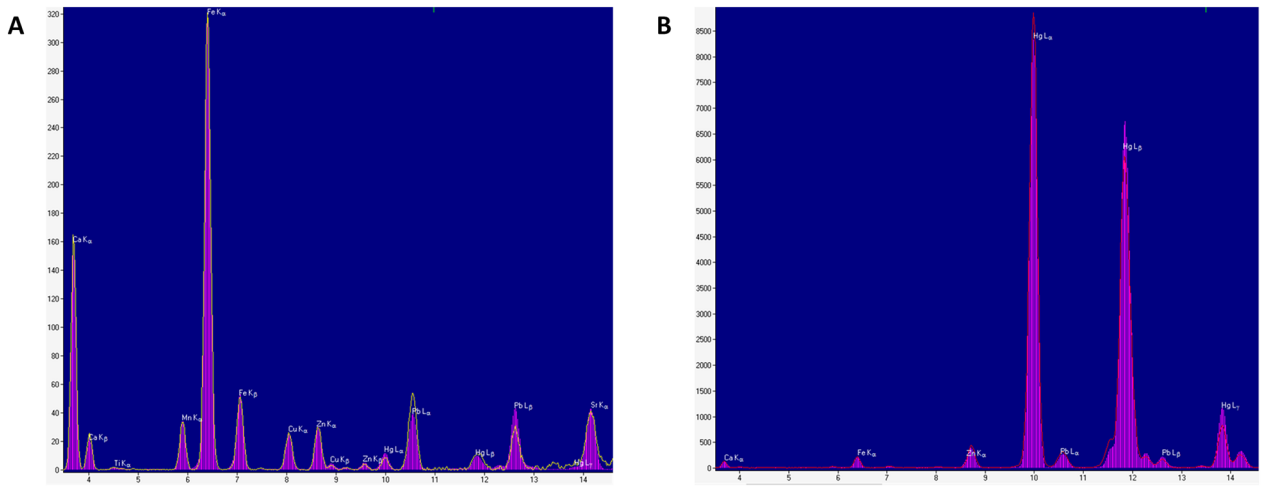


**Fig. 9** Comparison of the spectrum in the non-ink area **A** and in the red ink area **B** on page 183-1 (first part of the book). Both spectra have different counts range (up to 320 for **A** and up to 8500 for **B**

from the same area. The accelerating voltage in this case was 12 kV ("light spectrum") and no filter was used. The data collection took 300 s.

### XRF data evaluation

The ElvaX software tool was used to evaluate the data. The obtained spectra are quite complex and their evaluation must be approached with great caution. The XRF spectrometer used has a rhodium anode, therefore it does not enable the analysis of the presence of chlorine, whose K edges are in the same energy region as the L edges of rhodium. Sulphur detection is similarly problematic. During the evaluation, the spectra were measured in the red pigment-free paper regions which were compared with the paper containing red pigment regions.

The book contains three parts with visually different printing and paper. By evaluating the spectra in the inkless paper area, it was found that the paper material throughout the book is similar but not exactly the same. Calcium, iron, manganese, copper and zinc were found in all places; other elements were found in lower concentrations. In addition, however, we also found traces of mercury and lead in the paper area, which originate from ink abrasion and mercury diffusion. Note that such diffusion is well known, for example, for iron gall inks, see [7, 8]. Despite the aforementioned similarity in paper composition, minor differences were found. The paper of the title page contained less calcium and iron than the paper in the first and third part. It also lacked traces of mercury. The paper of the third part had the highest iron content, the paper of the first part the highest calcium content.

Subsequently, the ink analyses were carried out. The red ink showed an abundant presence of mercury and lead. Sulphur is also detectable. This finding confirms that the red ink is a vermilion-based pigment (cinnabarite). More precisely, quantitative analysis of the ink indicated that the red pigment is composed of 97% mercury sulphide and 3% lead, which is either an admixture in the ore or it was deliberately added during pigment preparation, see [41]. The spectrum directly from the Prospector instrument is shown in Fig. 9 for illustration. The spectrum of the paper on page 183 of the first volume of the book is shown in Fig. 9A; the spectrum of the area with red ink on the same page is shown in Fig. 9B. Note that mercury is also present in the paper, although only in a small proportion.

Comparison of the red ink spectra used in the first, second and third parts revealed that the ink from the third part showed a lower content of mercury but a higher content of lead (89% Hg, 11% Pb). Hence, the ink is based on the same pigment, but it cannot be ruled out that it is an ink from, for example, another workshop or a different batch.

No extra element was detected in the black ink area compared to red ink. From the analysis of tomographic sections from X-ray scanning and their comparison with photographs of specific pages of the book, it is immediately clear that only red ink causes significant attenuation due to the mercury and lead content. In Fig. 10 is a comparison of the front page with the inscription *Euchologion*. The red angel and part of the inscription are clearly visible on the tomographic section, while the black drawing is not. However, the representation of red ink in the book is high, so it is difficult to measure the spectrum


**Fig. 10** **A** Figure of the front page of the Euchologion. **B** tomographic section in approximately the same position, false colours in the order grey-yellow–red-purple correspond to increasing calculated CT density. Black ink creates no contrast

of black ink by XRF so that pulses from red ink on other pages do not leak. Measurements in the area of several pages with only black ink revealed a slightly higher concentration of mercury in the black ink than in the surrounding paper. Although the diffusion of mercury vapours into the whole book block is evident, its higher content in the black ink could also be attributed to the contamination of the ink during the print. Since no other significant element compared to paper was found, the composition of the black pigment cannot be determined. What can be said is that it is not a metal oxide pigment that can be detected by spectrometric analysis, which implies that it is very probably a common carbon-based pigment.

## Conclusions

Computed tomography performed on the TORATOM device enabled inspection of the internal structure of the relatively large historical book containing three parts, with outside dimensions 235 × 333 × 120 mm. Despite these dimensions, it was possible to perform a CT reconstruction with a voxel size down to 45 µm in order to improve the identification of the text from the red pigment and to improve the visibility of the tree rings needed for dendrochronological dating.

Based on detailed analysis of CT data with an intrinsic voxel size of 179 µm (given by detector pixel size divided by 1.1 × magnification), we found that there were no changes in sewing, attachment of cords or other components, nor was any evidence found of the removal of bookbinding elements. The only items bearing the marks of repair or replacement were the clasps, however it was known before. No parts are visible on the wooden boards indicating the earlier layers of attachment of the book boards. No distinct layers are visible in the spine to indicate the presence of fragments of recycled materials. Tomographic reconstruction before possible restoration provides detailed 3D information about the condition of an object and therefore enables the appropriate technological procedure to be chosen.

Another equally important insight was the demonstration of the possibility to read the text on individual pages throughout the book without having to remove the book from its protective cardboard box and open it.

This represents a significant advance in the possibilities of documenting and digitising texts in historical incunabula, for example those without cut signatures or where defects in the book binding make it impossible to open the book. Although the related procedure for reading a closed book was demonstrated on only one page, it can be extended to the entire book if required.

A key part of the research involved obtaining an image of the wooden book boards and tree rings for dendrochronological analysis. It was proven that book boards were made of oak felled sometime after 1608. The ring curve was dated using standard chronologies of oaks native to the Baltics.

X-ray fluorescence spectroscopic analysis of the black and red inks used in the book showed that the red ink is undoubtedly based on vermilion, a modification of mercury sulphide, and that significant amounts of lead were present, which is either a natural admixture in the mercury ore (cinnabarite) or was added during the extraction process of vermilion or it was added to change halftone of the pigment. The black ink used in the book also showed peaks of mercury and lead in the spectrum of the paper. It was concluded that these elements penetrate into the measured areas mainly due to the diffusion of mercury vapours released from the red pigment into the entire volume of the book block. This finding may be important for handling the book. The black pigment itself was found not to be based on black metal oxides and it is therefore probably a very common carbon-based pigment. It has been shown that the composition of the paper differs slightly in all three parts of the book.

**Acknowledgements**
This article was created through the institutional support of The National library of the Czech Republic for the long-term conceptual development of a research organisation provided by the Ministry of Culture of the Czech Republic. Furthermore, the research was supported by the European H2020 IPERION HS Project (Integrated Platform for the European Research Infrastructure ON Heritage Science) (GA 871034).

**Author contributions**
DV processed tomographic data to enable reading from a closed book and prepared tomographic data for dendrochronology, AK professionally processed materials for the research, performing analyses on the chemical and mechanical changes in samples after irradiation in order to protect the bookbinding accordingly, JN coordinated the research on the book and evaluated the outputs, interpreting these in terms of conservation and restoration research, RLK selected the manuscript for the research, interpreted the research results within the field of the book history, DN evaluated the outputs, interpreting them in terms of material composition and the technology of bookbinding production, PV coordinated the research, as well as participated in the evaluation of the results of the analyses and the interpretation of the conclusions, IK carried out the tomographic measurements on the book, as well as tomographic reconstruction and visualization, MV not only worked on the software for the tomographic scanner and on the tomographic visualizations, but also performed XRF measurements at selected places in the book, including the subsequent interpretation of the results, TK performed a dendrochronological analysis based on the acquired data, dating and determining the area of origin of the wood used for the book plates.

**Funding**
All sources of funding for the research are declared in the Acknowledgement.

**Availability of data and materials**
The datasets used and/or analysed during the current study are available from the corresponding author on reasonable request.

## Declarations

**Ethics approval and consent to participate**
The authors have permission to use all images in the article and have properly credited all sources and acknowledged all contributors. No portion of this article has been published or is pending publication with another journal in any form or language.

**Competing interests**
The authors have no competing interests that might be perceived to influence the results and/or discussion reported in this paper.

Received: 12 September 2023 Accepted: 5 March 2024
Published online: 13 March 2024

**References**

1. Duivenvoorden J, Käyhkö A, Kwakkel E, Dik J. Hidden library: visualizing fragments of medieval manuscripts in early-modern bookbindings with mobile macro-XRF scanner. Herit Sci. 2017. https://doi.org/10.1186/s40494-017-0117-6.
2. Starynska A, Messinger D, Kong Y. Revealing a history: palimpsest text separation with generative networks. IJDAR. 2021;24:181–95. https://doi.org/10.1007/s10032-021-00379-z.
3. Salerno E, Tonazzini A, Bedini L. Digital image analysis to enhance underwritten text in the Archimedes palimpsest. IJDAR. 2007;9:79–87. https://doi.org/10.1007/s10032-006-0028-7.
4. Zawacki AJ, Huskin KA, Davies H, Kleynhans T, Messinger D, Heyworth G. Fragments under the lens: a case study of multispectral versus hyperspectral imaging for manuscript recovery. Digital Philol A J Medieval Cult. 2023;12(1):123–43. https://doi.org/10.1353/dph.2023.0004.
5. Tachau KH. The king in the manuscript, the presentation inscription of the Vienna Latin bible Moralisée. Gesta. 2021;60:1. https://doi.org/10.1086/712635.
6. Turner NK, Patterson CS, MacLennan DK, Trentelman K. Visualizing underdrawings in medieval manuscript illuminations with macro-X-ray fluorescence scanning. X-Ray Spectrom. 2019;48:251–61. https://doi.org/10.1002/xrs.2956.
7. Kanngießer B, Hahn O, Wilke M, Nekat B, Malzer W, Erko A. Investigation of oxidation and migration processes of inorganic compounds in ink-corroded manuscripts. Spectrochimica Acta Part B: Atomic Spectroscopy. 2004;59:1511–6. https://doi.org/10.1016/j.sab.2004.07.013.
8. Gimat A, Michelin A, Massiani P, Rouchon V. Beneficial effect of gelatin on iron gall ink corrosion. Herit Sci. 2021. https://doi.org/10.1186/s40494-021-00593-2.
9. Pouyet E, Devine S, Grafakos T, Kieckheffer R, Salvant J, Smieska L, Woll A, Katsaggelos A, Cossairt O, Walton M. Revealing the biography of a hidden medieval manuscript using synchrotron and conventional imaging techniques. Analytica Chimica Acta. 2017;982:20–30. https://doi.org/10.1016/j.aca.2017.06.016.
10. Mercuri F, Cicero C, Orazi N, Paoloni S, Marinelli M, Zammit U. Infrared thermography applied to the study of cultural heritage. Int J Thermophys. 2015;36:1189–94. https://doi.org/10.1007/s10765-014-1645-x.
11. Sargan JD, Lockhart JL, Nelson A, Meert-Williston DL, Gillespie A. The ghosts of bindings: micro-computed X o-computed X-ray tomography for the study of bookbinding. Digital Philol A J Medieval Cult. 2022. https://doi.org/10.1353/dph.2022.0009.
12. Ensley JE, Tachau KH, Walsh SA, Zhang H, Simon G, Moser L, Atha J, Dilley P, Hoffman EA, Sonka M. Using computed tomography to recover hidden medieval fragments beneath early modern leather bindings. First results. Herit Sci. 2023. https://doi.org/10.1186/s40494-023-00912-9.

13. Albertin F. 2022, X ray tomography for manuscripts. Umanistica Digitale. 2022;6(12):39–64. https://doi.org/10.6092/issn.2532-8816/14399.
14. Van Noorden R. X-rays reveal words in Vesuvius-baked scrolls. Nature. 2015. https://doi.org/10.1038/nature.2015.16763.
15. https://new.manuscriptorium.com/hub/catalog/default/detail/single/manuscriptorium%7CAIPDIG-NKCRSKT9270RB3099_3ZF1DHC-cs?lang=en.
16. Herman GT. Filtered backprojection for divergent beams. In: Herman Gabor T, editor. Fundamentals of computerized tomography. London: Springer; 2009. https://doi.org/10.1007/978-1-84628-723-7_10.
17. Fíla T, Kumpová I, Jandejsek I, Kloiber M, Tureček D, Vavřík D. Utilization of dual-source X-ray tomography for reduction of scanning time of wooden samples. J Instrum. 2015. https://doi.org/10.1088/1748-0221/10/05/C05008.
18. Fíla T, Kumpová I, Koudelka P, Zlámal P, Vavřík D, Jiroušek O, Jung A. Dual-energy X-ray micro-CT imaging of hybrid Ni/Al open-cell foam. J Instrum. 2016. https://doi.org/10.1088/1748-0221/11/01/C01005.
19. Fila T, Vavrik D. A multi-axial apparatus for carrying out x-ray measurements, particularly computed tomography. European patent EP2835631. 2018.
20. Gimat A, Schoeder S, Thoury M, Dupont AL. Impact of the paper degradation state and constituents on its behavior during and after X-ray exposure. Preprint. 2021. https://doi.org/10.21203/rs.3.rs-1000597/v1.
21. International Atomic Energy Agency. Uses of ionizing radiation for tangible cultural heritage conservation. IAEA radiation technology series No. 6. Vienna: IAEA; 2017. p. 68–73.
22. Vadrucci M, Cicero C, Mazzuca C, Mercuri F, Missori M, Orazi N, Severini L, Zammit U. Effect of X-ray and artificial aging on parchment. Eur Phys J Plus. 2021;136:873. https://doi.org/10.1140/epjp/s13360-021-01766-5.
23. Dupont AL, Gimat A, Schoeder S, Thoury M, Lacombe SP. Short- and long-term effect of radiation damage in cotton paper. SOLEIL Highlights 2020, synchrotron SOLEIL. 2021. https://hal.science/hal-03423765.
24. Kazanskii A. Bezpečnost neinvazivního průzkumu využívajícího záření o specifické vlnové délce. Knihovna. 2022;33(2):78–95.
25. Catarina M. The alchemy of red mercury sulphide: the production of vermilion for medieval art. Dyes Pigments. 2014;102:210–7. https://doi.org/10.1016/j.dyepig.2013.10.041.
26. Stromer D, Christlein V, Martindale C, Zippert P, Haltenberger E, Hausotte T, Maier A. Browsing through sealed historical manuscripts by using 3-D computed tomography with low-brilliance X-ray sources. Sci Rep. 2018;8:15335. https://doi.org/10.1038/s41598-018-33685-4.
27. Dambrogio J, Ghassaei A, Smith DS, Jackson H, Demaine ML, Davis D, Mills D, Ahrendt R, Akkerman N, van der Linden D, Demaine ED. Unlocking history through automated virtual unfolding of sealed documents imaged by X-ray microtomography. Nat Commun. 2021;12:1184. https://doi.org/10.1038/s41467-021-21326-w.
28. Vavrik D, Antušková V, Chlumská Š, Kumpová I, Šefců R, Vopálenský M. Non-destructive exploration of Late Gothic panel painting using X-ray tomography and flattening of the reconstructed data. Eur Phys J Plus. 2023;138:618. https://doi.org/10.1140/epjp/s13360-023-04212-w.
29. Kumpova I, Vavrik D, Vopalensky M. Reading closed historical manuscripts using dual-source dual-energy X-Ray tomography. 8th Conference on Industrial Computed Tomography (iCT) Wels, Austria. e-Journal of Nondestructive Testing. 23(2). 2018. https://www.ndt.net/?id=21947.
30. Daly A. Non-invasive dendrochronological analysis of four book bindings "Missale Nidrosiense" Norway. 2019. MoK. https://doi.org/10.5281/zenodo.4355836.
31. Schweingruber FH. Microscopic wood anatomy. Eidgenössiche forschungsantalt für wald, schnee und landchaft, birmensdorf. 1990.
32. Kyncl J. Dendrochronologické datování dřeva (Dendrochronological dating of timber). In: Vinař a kol. Historické krovy II (Historical roof trusses II). Grada. 2005;156–170.
33. Cook ER, Kairiukstis LA. Methods of dendrochronology. Applications in the environmental sciences. Int Inst Appl Syst Anal. 1990. https://doi.org/10.1007/978-94-015-7879-0.
34. Baillie MGL, Pilcher JR. A simple cross-dating program for tree-ring research. Tree-Ring Bull. 1973;33:7–14.
35. Daly A, Tyers I. The sources of Baltic oak. J Archaeol Sci. 2022. https://doi.org/10.1016/j.jas.2022.10555.
36. Eckstein D, Wazny T, Bauch J, Klein P. New evidence for the dendrochronological dating of Netherlandish paintings. Nature. 1986;320:465–6.
37. Patlach ER, Kairiukstis LA. Methods of dendrochronology. Dodrecht, Boston, London: Kluwer Acad Publ; 1990.
38. Legrand S, Ricciardi P, Nodari L, Janssens K. Non-invasive analysis of a 15th century illuminated manuscript fragment: point-based vs imaging spectroscopy. Microchem J. 2018;138:162–72. https://doi.org/10.1016/j.microc.2018.01.001.
39. Van der Snickt G, De Nolf W, Vekemans B, Janssens K. μ-XRF/μ-RS vs. SR μ-XRD for pigment identification in illuminated manuscripts. Appl Phys A. 2008;92:59–68. https://doi.org/10.1007/s00339-008-4447-9.
40. Duran A, Perez-Rodriguez JL, Espejo T, Franquelo ML, Castaing J, Walter P. Characterization of illuminated manuscripts by laboratory-made portable XRD and micro-XRD systems. Anal Bioanal Chem. 2009;395:1997–2004. https://doi.org/10.1007/s00216-009-2992-5.
41. Nöller R. Cinnabar reviewed: characterization of the red pigment and its reactions. Stud Conserv. 2015;60(2):79–87. https://doi.org/10.1179/2047058413Y.0000000089.


## Publisher's Note